



Role of Nano- and Crystalline Silica to Accelerate Chemical Treatment of Problematic Soil

Nripojyoti Biswas, Ph.D., A.M.ASCE¹; Anand J. Puppala, Ph.D., P.E., D.GE, F.ASCE²; and Sayantan Chakraborty, Ph.D., A.M.ASCE³

Abstract: A research study was conducted to accelerate engineering property improvements by using novel silica-based coadditives along with a traditional calcium (Ca)-based stabilizer. Silica-based compounds, crystalline-silica (CS) rich waste product, and laboratory-grade nanosilica (NS) were used as coadditives with dolomitic hydrated lime to treat problematic expansive soil to study their efficacy in accelerating improvements in various engineering characteristics. The optimum dosages of the CS and NS additives with dolomitic hydrated lime were first determined based on unconfined compressive strength property, before and after capillary soaking. These dosages were subsequently corroborated by performing one-parameter and multiparameter statistical analyses. Using these optimized dosages, various engineering tests were performed on the treated soils. These tests included free-swell and linear shrinkage strains, unconfined strength with and without capillary soaking, and resilient modulus studies at curing periods of 0 (6 h), three, and seven days. Supplemental microstructural analyses were performed to gain insights into the factors responsible for the observed improvements in engineering properties. Test results indicated that treatment with hydrated lime and both silica-based coadditives is effective in stabilizing problematics soil as compared with lime treatment alone. Among the two silica-based coadditives, NS treatment provided comparatively higher accelerated improvements in the soil properties after seven days of curing than CS treatment. Mineralogical studies revealed that NS is more reactive than CS as a coadditive; hence, NS has been effective in providing equivalent long-term engineering strength gains while reducing swelling- and shrinkage-related volume-change properties in a relatively short time period. **DOI:** [10.1061/JGGEFK.GTENG-10999](https://doi.org/10.1061/JGGEFK.GTENG-10999). © 2023 American Society of Civil Engineers.

Introduction and Background

Transportation infrastructure and other lightweight structures built on problematic expansive subsoils suffer from several distresses induced by seasonal moisture fluctuations, including rutting, cracking, and differential heaving (Little 2000; Chittoori 2008; Puppala and Pedarla 2017; Chakraborty and Nair 2020). These damaged infrastructures require regular maintenance and rehabilitation work that account for several millions of dollars annually in the USA alone (Gomes Correia et al. 2016; Das 2018; Khan et al. 2020). Calcium-based additive treatment has been widely used for several decades in different parts of the world to stabilize expansive soils and prevent moisture-induced distresses when they are supporting civil infrastructure (Little et al. 2000; National Lime Association 2004; Puppala 2021). The addition of quick lime or hydrated lime to high-plastic clays improves workability and engineering properties

of the treated soil layers (Puppala et al. 1996; Bell 1996; Dash and Hussain 2012; Chakraborty et al. 2022; Jang et al. 2021).

The stabilization mechanisms for treatment of clayey soils with calcium (Ca)-based stabilizers can be primarily classified into two stages: an immediate modification stage and a time-dependent pozzolanic reaction phase. The modification stage includes cation-exchange, flocculation, and agglomeration reactions, which result in a decrease in soil plasticity and moisture-holding capacity of soil particles, reduction in the swell–shrink potentials, and an immediate improvement in the workability and strength properties. In the second stage, long-term strength gain occurs through pozzolanic reactions and the formation of cementitious products such as calcium-silicate-hydrate (C–S–H) and calcium-aluminate-hydrate (C–A–H) (Little et al. 2000; Mitchell and Soga 2005; Al-Rawas and Goosen 2006).

While these reactions enhance the engineering properties, the permanency of Ca-based stabilizer treatment has been a major cause of concern for researchers over the past several decades (Kennedy et al. 1987; McCallister and Petry 1992; Chittoori et al. 2013). Durability issues of stabilized soils not having appreciable amounts of sulfates and organic matter have been primarily attributed to moisture intrusion, leaching, carbonation, and exposure to extreme environmental conditions (Christopher et al. 2006; Chittoori et al. 2013; Aldaood et al. 2014; Chakraborty and Nair 2020). Leaching, carbonation of stabilizers, and exposure to extreme environmental conditions are time-dependent phenomena, and their deleterious impacts are not observed immediately. In contrast, moisture exposure during the early curing periods has been reported to cause immediate degradation in engineering properties of lime-treated soils (Dempsey and Thompson 1968; Little 1996). Strength losses close to 40% of unsoaked strength properties have been reported when moisture intrusion has occurred during the early ages of curing (Dempsey and Thompson 1968; Little 1996; Little and Nair 2009). In contrast, less than 10% of unsoaked

¹Postdoctoral Researcher, Zachry Dept. of Civil and Environmental Engineering, Texas A&M Univ., College Station, TX 77840. ORCID: <https://orcid.org/0000-0001-5548-1292>. Email: nripojyoti.biswas@tamu.edu

²Professor and A.P. and Florence Wiley Chair, Zachry Dept. of Civil and Environmental Engineering, Texas A&M Univ., College Station, TX 77840 (corresponding author). ORCID: <https://orcid.org/0000-0003-0435-6285>. Email: anandp@tamu.edu

³Assistant Professor, Dept. of Civil Engineering, Birla Institute of Technology and Science, Pilani, Rajasthan 333031, India. ORCID: <https://orcid.org/0000-0002-6809-5953>. Email: sayantan.chakraborty@pilani.bits-pilani.ac.in

Note. This manuscript was submitted on April 25, 2022; approved on February 8, 2023; published online on April 24, 2023. Discussion period open until September 24, 2023; separate discussions must be submitted for individual papers. This paper is part of the *Journal of Geotechnical and Geoenvironmental Engineering*, © ASCE, ISSN 1090-0241.

strength loss has been observed after a significant level of pozzolanic reaction due to the formation of cementitious compounds after prolonged curing of 28 days (Little and Nair 2009).

Besides the curing time, the extent of strength loss in lime-treated soils depends on the soil type, clay mineralogy, and lime dosage (Kennedy et al. 1987; McCallister and Petry 1992; Chittoori et al. 2013). For a given problematic soil type, the kinetics of the pozzolanic reactions between clay minerals and the stabilizer as well as the formation of cementitious compounds cannot be altered at room temperature conditions without increasing the stabilizer dosage or introducing an additive that can accelerate the pozzolanic reaction. Selecting high stabilizer dosages is usually uneconomical and even counterproductive from a sustainability point of view, as reported by previous research studies (Bell 1996; Kumar et al. 2007; Dash and Hussain 2012). As a result, past researchers have attempted to use several other alternatives, including the addition of coadditives with primary stabilizers to improve the performance of the treated soils.

Different coadditives derived from the industrial waste materials such as ground granulated blast furnace slag, Class C or Class F fly ash (FA), cement kiln dusts, lime kiln dusts, rice husk ash, bagasse fibers, and silica fumes have been used along with lime to enhance the performance of the treated soils (Misra 1998; Wild et al. 1999; Çokça 2001; Hilbig and Buchwald 2006; Peethamparan et al. 2008; Chen et al. 2009; Kumar and Gupta 2016; Li et al. 2019). These coadditives furnish additional pozzolanic phases of aluminates and amorphous and crystalline phases of silicates, which react in a high alkaline environment to form cementitious compounds (Bakharev et al. 1999; Kukko 2000; Brough and Atkinson 2002; Behnood 2018). Even though the majority of these studies indicate the potential benefits of adding these coadditives for accelerated strength gains in lime-treated soils, researchers are continuously striving to identify novel coadditives that could be used with hydrated lime for enhancing the reaction rates in the chemically treated soils.

In the past decade, there has been a major focus on the use of nanomaterials to nanotechnologies for the enhancement of the properties of cementitious reactions. The application of amorphous nanosilica to cement composites improves the microstructure by developing a denser matrix by filling pores and enhancing the rate of the pozzolanic reactions (Sobolev et al. 2009; Stefanidou and Papayianni 2012; Givi et al. 2013). The application of nanosilica has resulted in significant improvements of several engineering properties, such as reducing volumetric strains and improving the compaction characteristics and compressive strengths of the treated soils (Taha and Taha 2012; Bahmani et al. 2014, 2016).

Recently, the use of crystalline-silica-rich quarry fines to stabilize sulfate-rich expansive soil has indicated sustainable solutions to the landfill problems associated with the disposal of quarry fines dust (Chakraborty et al. 2022; Biswas et al. 2021). Several research studies have shown that the crystalline-silica fines have the ability to participate in cementitious reactions when subjected to long-term curing or curing at elevated temperature conditions (Sivapullaiah and Moghal 2011; Dash and Hussain 2012, 2021). Amorphous nanosilica and crystalline silica-rich quarry fines have excellent potential to be used for various engineering applications (Lamb 2005; Puppala et al. 2012; Ingalkar and Harle 2017). However, limited studies have either focused on or directed toward enhancing the rate of chemical reactions in lime-treated soils. Furthermore, none of the studies using silica-based admixtures have focused on improving short-term strength and durability in lime-treated soils. Therefore, it was hypothesized that adding suitable silica-based coadditives with traditional Ca-based stabilizers could accelerate the formation of cementitious products and prevent significant

moisture-induced strength losses in the treated soils during the early curing stages.

This research study was undertaken to investigate and then evaluate the applicability of silica-based co-additives with traditional Ca-based lime stabilizers for rapid stabilization of problematic high-plasticity clayey soil. The rapid improvement in soil properties encompasses quick improvements in strength, moisture-susceptible durability, stiffness and swell–shrink behavior due to the application of silica-based coadditives. A comprehensive testing program, including engineering and microstructural studies, was designed and performed on the lime-treated soil (L), lime and crystalline silica-treated soils (L + CS), and lime and nanosilica-treated soils (L + NS) combinations. The impacts of coadditive dosage and behavior after exposure to moisture intrusion for the curing periods of zero (6 h), three, and seven days were studied and addressed. Additionally, mineralogical and microstructural analyses were performed to understand the possible reasons for observed changes in the engineering properties of the treated soils stabilized with different coadditives. A statistical optimization framework was used to determine the statistical significance of different dosages of coadmixtures on the enhancements of strength properties of the treated soils and subsequently determine the optimum coadditive dosages.

The subsequent sections present the stabilizer additive and co-additive materials used, the engineering and microstructural studies undertaken, and later sections cover the development of the statistical framework and analyses of test results. The analyses and discussions on the engineering and microstructural results are used to develop comprehensive treatment guidelines and assessments of benefits from a sustainability perspective.

Materials and Test Methods

Material Characterization

The soil for this research investigation was obtained from a pavement construction site near the Paris District in Texas, USA. The specific surface area of the soil, determined by the methylene blue spot test, was obtained approximately $75 \text{ m}^2/\text{g}$. The soil was classified as a low-sulfate soil with soluble sulfate content of 400 ppm, per Tex-145-E (Texas DOT 2005). The basic soil characterization results in accordance with respective standards [ASTM D854-14 (ASTM 2016), ASTM D4318-17e1 (ASTM 2018c), ASTM D7928-21e1 (ASTM 2021a), ASTM D2487-17 (ASTM 2020), ASTM D698-12 (ASTM 2021b), ASTM D4546-21 (ASTM 2021c), Tex-107-E (Texas DOT 1999)] and grain size distribution are shown in Table 1 and Fig. 1, respectively. An x-ray fluorescence (XRF) study was performed on the soil specimen to study the chemical composition; the results are presented in Table 2. A low concentration of soluble sulfates was observed in the untreated

Table 1. Basic characterization of clayey soil used in this research

Property	Magnitude
Specific gravity (ASTM D854-14)	2.72
Liquid limit (ASTM D4318-17e1)	60
Plastic limit (ASTM D4318-17e1)	27
Plasticity index (ASTM D4318-17e1)	33
Silt (%) (ASTM D7928-21e1)	41.7
Clay (%) (ASTM D7928-21e1)	51.2
USCS soil classification (ASTM D2487-17)	CH
Maximum dry unit weight (kN/m^3) (ASTM D698-12)	16.25
Optimum moisture content (%) (ASTM D698-12)	19
Vertical free swell strain (%) (ASTM D4546-21)	15.7
Linear shrinkage (%) (Tex-107-E)	14.5

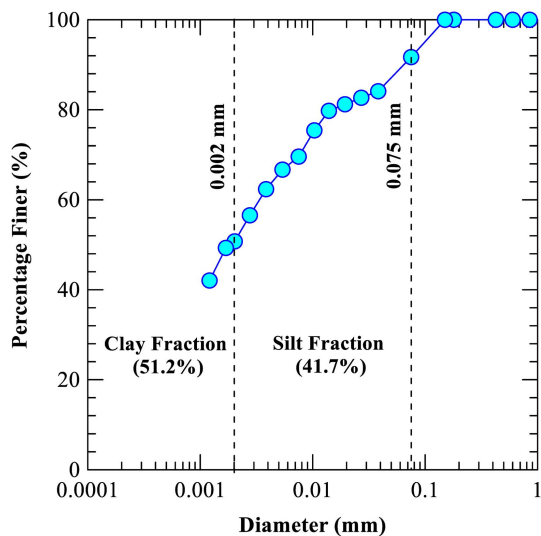


Fig. 1. Grain size distribution of untreated CH soil.

Table 2. Chemical composition of CH soil and Ca-based stabilizer from XRF studies

Chemical composition	Mass (%)	
	CH soil	Ca-based stabilizer
Silicon oxide (SiO_2)	28.77	4.43
Aluminum oxide (Al_2O_3)	23.48	9.45
Ferric oxide (Fe_2O_3)	7.24	0.33
Calcium oxide (CaO)	36.95	51.49
Magnesium oxide (MgO)	1.68	28.29
Sulphur trioxide (SO_3)	0.11	0.01
Sodium oxide (Na_2O)	0.03	0.12
Potassium oxide (K_2O)	1.68	0.01
Loss of ignition	0.06	5.87

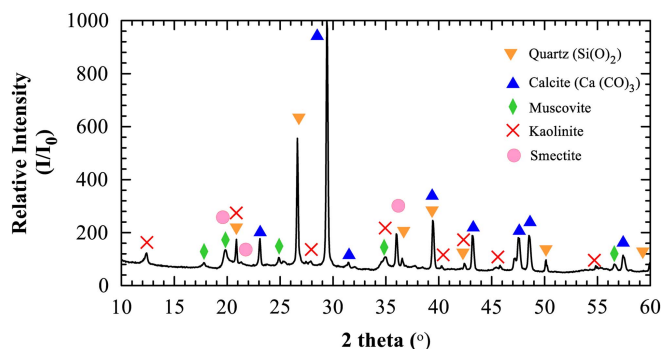


Fig. 2. X-ray diffractogram of untreated soil.

soils using the XRF test; these results corroborated the results obtained from the colorimetric method [Tex-145-E (Texas DOT 2005)]. The XRF study also indicated that the soil has a major concentration of Ca oxides, in addition to the presence of Si and Al oxides. This was also confirmed with the x-ray diffraction (XRD) study performed on the untreated soil, as shown in Fig. 2. The x-ray diffractogram of the natural soil indicates that the soil is primarily composed of kaolinite, muscovite, quartz, smectite, and calcite minerals.

Dolomitic-hydrated lime conforming to ASTM C977-18 (ASTM 2018a) standard method was procured from a local supplier and used as the primary stabilizer for the subsequent studies. The chemical composition of the lime stabilizer was also analyzed using XRF, as presented in Table 2. In this study, the performance of two different coadmixtures was compared when added with a Ca-based stabilizer to accelerate the chemical reactions during treatment. The first coadditive was an amorphous silica-based product, which is a commercially available nanosilica (NS) solute. The NS solute has a dilution ratio of 50%, specific surface area of $140 \text{ m}^2/\text{g}$, and a molecular weight of 60.08 g/mol. The second coadditive used was crystalline silica (CS) fines similar to quarry fines. Locally available sand was crushed, pulverized, and wet-sieved through a US#200 sieve, and the fine fraction was subsequently used in this study and is termed as CS fines. The next section discusses different engineering and microstructural studies as well as statistical methods used for the analysis of results obtained from testing the treated soil groups.

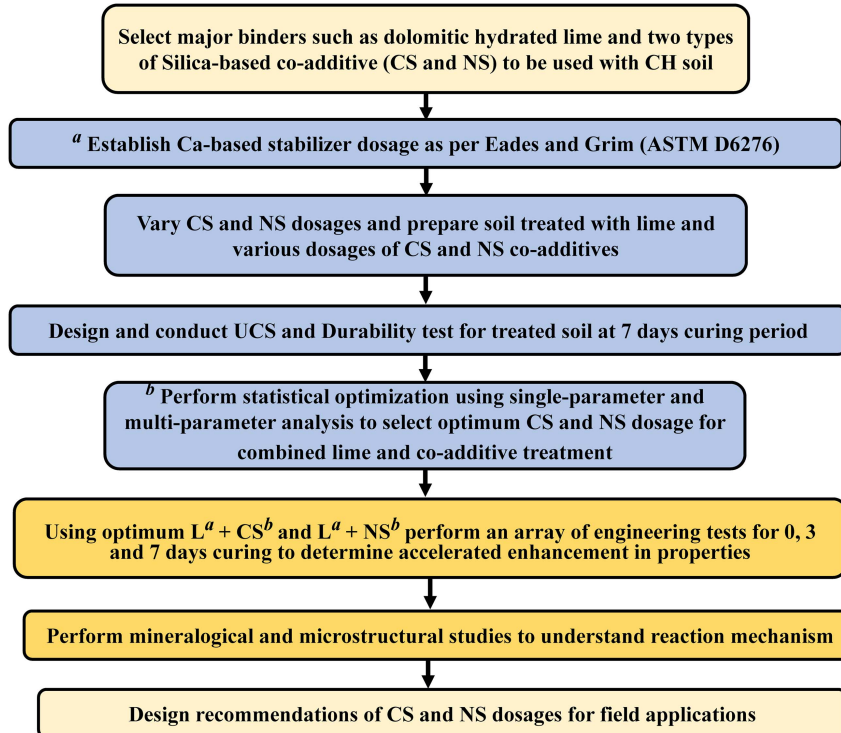
Experimental Program

In this program, engineering, chemical, and microstructural studies were performed to study and understand the effects of the silica-based coadditives when mixed with a traditional Ca-based stabilizer. The overall research approach outlining all tasks is presented in Fig. 3. The steps involved in the stabilizer mix design of combined dolomitic hydrated lime either with crystalline silica or with nanosilica coadditive is organized as follows: first, the dosage of lime stabilizer was optimized based on pH results, to determine the minimum lime requirement for sustaining long-term pozzolanic reactions; and second, statistical optimization analysis of engineering test results was attempted to study the optimized NS and CS levels when mixed with optimum lime dosage determined in the first step. A second approach was performed on unconfined compressive strength (UCS) property and retained strengths after capillary soaking of treated soil specimens after seven days of curing period. The improvements in the UCS and the retained strengths after capillary soaking are the key parameters considered here to assess the efficacy and durability of the present soil stabilization methods.

Using the optimum dosages of both coadditives with dolomitic lime, other engineering tests such as swelling- and shrinkage-related strains, and resilient moduli studies were performed after different curing periods of zero, three, and seven days. The improvements in strength and durability were analyzed over the same curing periods. Final stabilization designs were made based on comprehensive analyses of engineering, chemical, and microstructural studies performed on the treated geomaterials. More details of these investigations are provided here in later sections.

LMO Design and Specimen Preparation

The lime modification optimum (LMO) was determined by Eades and Grim's pH test method in accordance with ASTM D6276-19 (ASTM 2019) method. About 6% lime by the dry weight of the soil was required to attain a pH value of 12.40 for all treated soil groups, and this dosage was used as the LMO for this study. For the lime-treated soil and lime-CS treated soil, dry soil or dry soil with crystalline silica and lime were uniformly mixed to the desired proportions. Thereafter, water was added to the dry soil-binder mixtures and blended uniformly to produce a homogeneous treated soil mixture. In the case of treatment with NS additive, both soil and lime were uniformly mixed in the dry state. The NS solute was mixed with the required molding water and stirred continuously for 5 min using a magnetic stirrer before adding the water-NS solution to the dry soil-lime mixture. This was done to ensure that nanoparticles were uniformly distributed within the treated soil matrix.



Note: CS-Crystalline Silica; NS-Nano Silica; L-Dolomitic Hydrated Lime; CH-High PI Clay; ^a = Specimens with optimum lime content; ^b = Specimens with optimum co-additive content

Fig. 3. Research flow with tasks performed in the stabilization design.

The homogeneous soil mixtures were then statically compacted to prepare soil specimens required for unconfined strength, swell strain, and resilient modulus tests. Soil specimens were compacted at a target dry unit weight of 14.67 kN/m³ and a moisture content of 20%, determined in accordance with the ASTM D558-04 (ASTM 2010) method. The treated soil specimens for different co-additive groups were compacted at the same dry unit weight and moisture content condition of only lime-treated soils to ensure a similar zero-day strength condition.

Optimization of Coadditive Dosages and Strength Studies

Optimization of silica dosages was necessary, considering the economic aspects and engineering performance requirements. For crystalline silica (CS) coadditive, four dosages were selected for the initial trials (X%): 5%, 10%, 15%, and 20% of the dry weight of the soil. Similarly, for NS coadditive, four dosages (Y%) of 0.25%, 0.5%, 1.0%, and 2.0% by the dry unit weight of the soil were considered. Six cylindrical soil specimens [diameter = 33 mm; aspect ratio: 2(H):1(D)] of each treated soil groups were prepared using the static compaction method, demolded, and cured for seven days in a hermetically sealed chamber to ensure a relative humidity close to 100% at a temperature of 23 ± 2°C. Triplicate specimens for each soil group were tested in accordance with the ASTM D5102-09 (ASTM 2018b) method for unsoaked strength and strength after subjecting the treated soil specimens for a capillary soaking period of 48 h. The unsoaked strength of the curing specimens provided insights into the extent of the pozzolanic reactions in the different treated soil groups. In contrast, the strength properties of the capillary-soaked soil specimens facilitated understanding of the effects of moisture intrusion on strength properties of

stabilized soil specimens, and these results also provided an indirect measure of the durability of the treated soil groups prepared after seven-day curing period.

The statistical significance of adding dolomitic-lime alone and dolomitic-lime mixed with different dosages of silica admixtures with the untreated soil on unsoaked and capillary soaked strength parameters was determined by using factorial experiments (Tukey HSD, Scheffe, and Bonferroni tests). These experiments are useful in understanding if the means of a dependent variable are significantly different from one another. The level of significance of all experimental values was chosen as 0.05 based on a 95% confidence interval. The one-factor experiments were based on the assumed null hypothesis that there is no significant difference between means of the groups. Three measures of variability were used for the analysis of variance in the one-factor test. These are

$$SST = \sum_{i=1}^k \sum_{j=1}^n (y_{ij} - \bar{y}_{..})^2 \quad (1)$$

$$SSA = \sum_{i=1}^k (\bar{y}_{i..} - \bar{y}_{..})^2 \quad (2)$$

$$SSE = \sum_{i=1}^k \sum_{j=1}^n (y_{ij} - \bar{y}_{..})^2 \quad (3)$$

where SST = total sum of squares; SSA = treatment sum of squares; SSE = error sum of squares; y_{ij} = j th observation from i th treatment; n = number of specimens per treatment; k = number of treatments;

$\bar{y}_{..}$ = mean of nk observations; and \bar{y}_i = mean of all observations in the specimen from i th treatment.

After performing the single factor analysis, the statistical significance of the differences among mean UCS values of the group was determined by multiple comparison tests. Multiple comparison tests are performed when the F -ratio becomes statistically significant. The F -ratio is defined as a tool to understand if the variance between the means of two populations (treated soil groups) is significantly different. Three tests, i.e., Tukey HSD, Scheffe, and Bonferroni multiple parameter tests, were performed in this analysis. Multiple comparison tests have been used to determine the p -values between the lime-treated soil group and the lime with co-additive treated soil groups. The p -values from multiple comparison studies provided insights regarding a particular treatment that caused a significant difference between the control group (lime-treated soil) and test groups' (lime and coadditives treated soils) mean UCS values. The selection of the optimum coadditive silica dosage was based on the statistical significance of the unconfined strength of different coadditives dosages as well as retained treated soil strength after moisture conditioning.

The optimized dosages of all stabilizer groups, including dolomitic lime, CS, and NS, were subsequently used for comprehensive evaluations of temporal strength and durability, swell–shrink related soil strain changes, and resilient modulus studies of soils modified with optimized dosages over three curing periods.

Swell–Shrinkage Strains and Resilient Modulus Studies

Swell and shrinkage strain characteristics of the untreated and treated soil specimens were measured using the 1D free-swell strain test and linear shrinkage strain test for three curing periods of zero, three, and seven days, respectively. These tests provided information on the improvements in the moisture-induced strains due to the application of the coadmixtures through the possible formation of cementitious phases. Specimens for swell–strain tests were statically compacted in a mold of 63.5 mm diameter and 25.4 mm height and cured similar to the UCS test specimens. At the end of curing period, specimens were inundated with water flow. Free swell strain values were measured under a surcharge of 1 kPa in accordance with ASTM D4546-21 (ASTM 2021c). For the shrinkage test, the homogenous treated soil mixtures were stored separately in a sealed chamber and cured in a similar method as other compacted soil specimens. After each target curing period, cured soils were mixed with water to reach a consistency similar to that attained at the liquid limit. Consequently, the wet soil was placed in a greased mold (19 × 19 × 127 mm) and gently jarred to assist the uniform flow of soil and remove any entrapped air. The linear bar shrinkage test was performed following the Texas Highway Agency guidelines outlined in the Tex-107-E (Texas DOT 1999) method.

In addition to evaluating the strength and swell–shrink strain properties of the various soil groups, repeated load triaxial tests (RLTT) were performed to evaluate the resilient moduli properties. The resilient modulus (M_R) value is a characteristic parameter needed in mechanistic-empirical pavement design for 1993 AASHTO (1993) pavement design methods. Resilient moduli properties are important to assess the ability of untreated and treated soils to withstand repeated loading conditions in the field and transfer these loads to underlying soils without those layers undergoing permanent deformations. Duplicate specimens of 71 mm diameter and 146 mm height were prepared for all untreated and treated soil groups, and RLTTs were performed in accordance with the AASHTO T 307 (AASHTO 2003) standard test method. Details of the engineering test results and discussions are provided in the subsequent sections.

Mineralogical and Microstructural Studies

Specimens of untreated and treated soils were subjected to field emission scanning electron microscopy (FESEM) studies for visual identification of the cementitious phases. The identification of new cementitious phases provided insights into the microstructural changes responsible for the enhancements of the macrostructural properties after the coadditive treatments. Since the primary focus of this study was to understand the efficacy of coadditives on engineering properties, any changes in the behavior of the pure silica-based coadditives when treated with Ca-based stabilizers could help to understand the primary factors for the observed macrostructural changes. Therefore, additional investigations using XRD studies were undertaken on silica-based coadditives treated with dolomitic-hydrated lime.

XRD studies were performed on CS- and NS-coadditives uniformly mixed with Ca-based stabilizers at different curing periods. The dry samples were pulverized and sieved through a 75 μm sieve. The powder samples were prepared in a 51.5 mm diameter polymethyl methacrylate (PMMA) holder with a height of 8.5 mm using the backloading technique. The PMMA holder with powder sample was loaded on to the XRD instrument and subjected to Cu- $\text{K}\alpha$ radiation with a wavelength of 1.54 nm operating at current of 30 kV and 10 mA over 2θ range of 10° to 60°, with a step size of 0.02° and 0.5 s/step. International Centre for Diffraction Data was used for the identification of the minerals present in the specimen based on the location of characteristic x-ray diffraction peaks. The diffraction patterns observed over different curing periods for lime-NS- and lime-CS-treated specimens were studied comprehensively. The formation of new peaks and relative changes in the existing peak intensities of the diffractograms were used to detect the formation of new chemical reaction products and other cementitious phases.

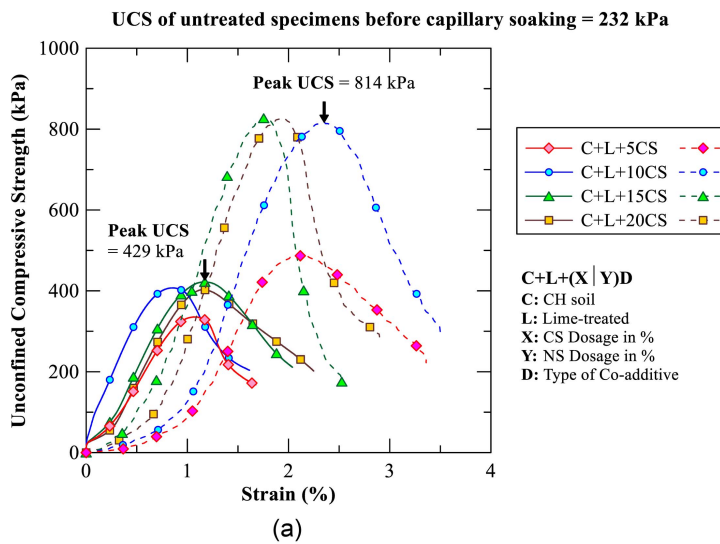
Analysis of Engineering Test Results

Optimization of CS and NS Dosages

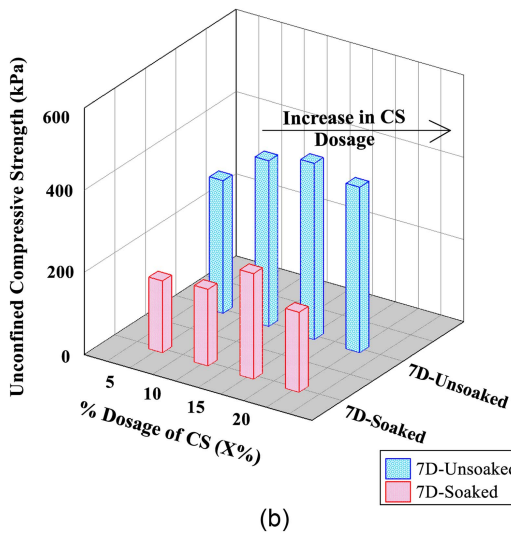
The untreated soil exhibited average unconfined strengths of 232 and 25 kPa before and after capillary soaking, respectively. These results indicated that the untreated soil is not durable and crumble when subjected to moisture intrusion during capillary soaking studies, reconfirming the need for chemical treatment.

Figs. 4(a–c) present the treated UCS values for both lime-CS and lime-NS specimens after curing for seven days. For lime-treated specimens, the UCS values after seven-days curing were recorded as 498 and 147 kPa, before and after 48 h of capillary soaking, respectively. Fig. 4(a) presents the UCS values for different CS dosages when mixed with dolomitic lime and subjected to seven days of curing. Initially, with an increase in CS dosage, there was an increase in the unsoaked strength; however, beyond 15% of CS dosage, there was no increase in the strength. The presence of a silica coadditive source has helped in the development of additional cementitious phases, which might have been responsible for providing the additional strength to the treated soil. However, beyond certain optimum dosage, CS might have replaced the original in situ soil, which is a major source of silicates and aluminates, to form cementitious reaction products in an alkaline environment. Therefore, an overreplacement of the in situ native soil with the crystalline silica source could potentially retard the strength gains.

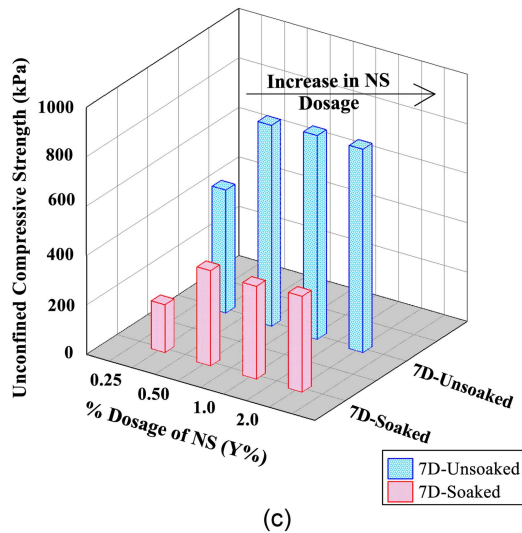
Similarly, it can be observed that, with an increase in NS dosage, there is a subsequent increase in the UCS values for the seven days cured specimens. However, beyond 0.5% of NS dosage, the strength gain was small and negligible. NS contains amorphous



(a)



(b)



(c)

Fig. 4. Optimization of coadditive dosage (a) unsoaked strength for different dosage after seven-day curing period; and soaked strength after capillary soaking for (b) CS treatment; and (c) NS treatment.

silica particles that are capable of uniformly mixing with the soil, thereby providing an additional source of reactive silica for cementitious reaction products. Mineralogical studies performed on the same treated soils were later used to corroborate these observations.

After subjecting the treated soil specimens to capillary soaking and then testing them as a part of durability studies, results showed that there was a considerable loss of strength for the seven-days cured soil specimens [Figs. 4(b and c)]. In the case of the lime and CS-treated soil group, the retained strength was maximum for 15% CS-treated specimens. Due to the moisture intrusion in the early curing period, the cementitious bonds formed are generally weak in nature. The formation of additional cementitious phases resulted in 60% strength retention as compared with unsoaked strength. It was, however, noted that, with higher replacement of in situ native soil with CS dosages, the retained strengths were decreased (<50%). This could be primarily attributed to an increased replacement of the cohesive soil by a cohesionless CS counterpart; during moisture ingress, the loss of the unconfined strength occurred due to weakening of the cementitious bonds and moisture susceptibility of cohesionless particles (Han and Vanapalli 2016).

For the NS-treated soils, the 0.5% NS dosage retained maximum strength for the seven-day cured specimens. C—S—H being

a hydrophilic mineral, excessive formation of C—S—H compounds could lead to an increase in water absorption when subjected to the capillary soaking process (Dash and Hussain 2012; Chakraborty and Nair 2017). An increase in water absorption could possibly lead to rapid loss of strength as compared with unsoaked treated soils. It was necessary to compare the seven-days strength of the treated soil using both statistical factors and engineering judgment such that, together, they can be used to determine the most optimized dosages of the coadditives for modifying such soils. The next section discusses the statistical approach adopted for optimization of the coadditive dosage.

One-Factor Experiments

The optimization of the dosage of admixture treatment was performed using the statistical framework discussed in the earlier section. Before subjecting the data set to one-factor experiments, the initial checks of normality and homogeneity were performed on the test data (Table 3). After the initial assumptions were satisfied, the population data were subjected to one-factor tests, and these results are presented in Table 4. The one-factor tests were initially performed separately between the untreated and C + L soils (T_1), untreated and C + L + XCS soils (T_2), and untreated

Table 3. Check for initial assumptions

Assumption	Parameter	Values	Comments
Normality	Kolmogorov-Smirnov statistic	0.206	
	p-value	0.136	Values are normally distributed
Homogeneity	Levene's statistics	1.007	
	p-value	0.467	Values are homogeneous

and C + L + YNS soil (T_3) (where X and Y are different dosage percentages of CS and NS coadditives, respectively). The first experiment, T_1 , indicated that the *p*-value is less than the assumed level of significance (<0.05). This showed a statistically significant difference between the mean UCS values of the untreated and lime-treated group. Similar observations were noted for T_2 and T_3 experiments, indicating that at least one of the mean strengths of the treated soil groups (for both experiments, T_2 or T_3) was significantly different from the means of the untreated control soil group. Hence, the treatment of soil improves its strength due to the formation of cementitious reaction products; therefore, the significant difference in mean values between the groups was noted.

Subsequently, the null hypothesis was tested on the remaining three groups of specimens, i.e., between the C + L and C + L + XCS soils (T_4), and C + L and C + L + YNS soils (T_5). From

the one-factor tests, it was noted that adding coadditives with lime has significantly affected the seven-days unsoaked strength. The *p*-values between lime-treated soil and lime and CS-treated soil (T_4), even though it is statistically significant, it primarily occurred because the average strength from lime treatment was around 550 kPa, and it was considerably higher than the average strength of 390 kPa for the lime and CS-treated soil. In the case of the soil treated with lime and NS (T_5), the average strength values were much higher (740 kPa) than lime-treated soil alone (550 kPa); hence, it affected the sample mean UCS values, and, subsequently, the *p*-values show statistically significant difference.

Optimization of Coadditive Dosage

From the one-factor experiments, it was evident that the addition of coadditives (either CS or NS) significantly affected the unsoaked strength over lime treatment alone after seven days of curing. However, one-factor experiments failed to provide conclusive evidence regarding the optimum dosage of either CS or NS, which might have a significant influence on the differences of mean UCS values as compared with lime-treatment alone. Hence, multiple comparison experiments were performed to understand the effects from different dosages of silica coadditives (CS or NS), having significant influence over lime-treated soil results (Tables 5 and 6).

The multiparameter analysis was initially tested on unsoaked strengths for lime and CS groups after seven days of curing, as shown in Table 5. The Tukey HSD test was unable to provide any definitive conclusions for this set of tests and their results. However, from Scheffe and Bonferroni *p*-values, it was observed that,

Table 4. Analysis of variance using one-factor experiments for the unsoaked strength of different soil groups

Specimen groups	Source of variation	SS	D _f	MS	F	p-value	F-crit
Untreated and C + L (T_1)	Between groups	106,667	1	106,667	35.9	3.90×10^{-3}	7.708
	Within groups	11,876.7	4	2,969.2			
	Total	118,543	5				
Untreated and C + L + XCS (T_2)	Between groups	78,791.1	4	19,697.7	180.2	2.85×10^{-9}	3.478
	Within groups	1,093.3	10	109.3			
	Total	79,884.4	14				
Untreated and C + L + YNS (T_3)	Between groups	852,878.7	4	213,219.7	938.2	7.94×10^{-13}	3.478
	Within groups	2,272.6	10	227.2			
	Total	855,151.3	14				
C + L and C + L + XCS (T_4)	Between groups	47,537.7	4	11,884.4	9.9	1.64×10^{-3}	3.478
	Within groups	11,962	10	1,196.2			
	Total	59,499.7	14				
C + L and C + L + YNS (T_5)	Between groups	373,412	4	93,353	71	2.65×10^{-7}	3.478
	Within groups	13,141.3	10	1314.1			
	Total	386,553	14				

Table 5. Multiple comparison statistical studies on unsoaked strength

Groups		Tukey HSD p-value	Scheffe p-value	Bonferroni p-value
Control group (mean, kPa)	Test group (mean, kPa)			
	C + L + 5CS (323.3)	1.005×10^{-3}	1.842×10^{-3}	1.003×10^{-3}
	C + L + 10CS (403)	43.079×10^{-3}	80.367×10^{-3}	69.125×10^{-3}
	C + L + 15CS (429.7)	180.718×10^{-3}	276.191×10^{-3}	346.473×10^{-3}
C + L (498.7)	C + L + 20CS (403)	43.079×10^{-3}	80.367×10^{-3}	69.125×10^{-3}
	C + L + 0.25NS (498.3)	899.995×10^{-3}	999.897×10^{-3}	20.535
	C + L + 0.5NS (812.7)	1.005×10^{-3}	8.989×10^{-9}	1.803×10^{-10}
	C + L + 1NS (825.3)	1.005×10^{-3}	4.578×10^{-9}	8.976×10^{-11}
	C + L + 2NS (823.3)	1.005×10^{-3}	1.789×10^{-9}	3.410×10^{-11}

Table 6. Multiple comparison statistical studies on soaked strength

Groups		Tukey HSD <i>p</i> -value	Scheffe <i>p</i> -value	Bonferroni <i>p</i> -value
Control group (mean, kPa)	Test group (mean, kPa)			
	C + L + 5CS (175.0)	1.613×10^{-2}	3.319×10^{-2}	2.423×10^{-2}
	C + L + 10CS (182.3)	3.221×10^{-3}	7.447×10^{-3}	4.528×10^{-3}
	C + L + 15CS (255.9)	1.005×10^{-3}	4.506×10^{-7}	1.939×10^{-7}
C + L (148.1)	C + L + 20CS (195.7)	1.005×10^{-3}	6.400×10^{-4}	3.280×10^{-4}
	C + L + 0.25NS (196.4)	8.603×10^{-3}	1.863×10^{-2}	1.254×10^{-2}
	C + L + 0.5NS (385.3)	1.005×10^{-3}	2.219×10^{-8}	9.342×10^{-9}
	C + L + 1NS (376.0)	1.005×10^{-3}	3.237×10^{-8}	1.365×10^{-8}
	C + L + 2NS (391.3)	1.005×10^{-3}	1.715×10^{-8}	7.212×10^{-9}

at 5% CS dosage, the *p*-values are less than 0.05, implying a significant difference between the means of control and test groups. This outcome was recorded because the 5% CS dosage resulted in lower strength in comparison with lime treatment. This could be primarily attributed to the partial replacement of alumino-silicate-rich clay minerals from dry soil as well as insufficient addition of crystalline counterparts to the soil. With an increase in CS dosage (10%, 15%, and 20%), even though there is an increase in the unsoaked strength of the soil, the difference in the mean values were insignificant within the groups (10%, 15%, and 20%). Therefore, for determining optimum dosage of CS coadditive, the effects of moisture intrusion on retained strength was tested using multiparameter analysis, as shown in Table 6. It was observed that all retained strengths for C + L + XCS soils have significant difference between the means as compared with only lime-treated soil. Consequently, in addition to the statistical outcomes, engineering judgment was used to select an optimum dosage for soil treatment [Fig. 4(b)]. From Fig. 4(b), it could be observed that 15% CS retained the maximum strength, i.e., 60% as compared with other dosages. Therefore, 15% CS dosage was considered as optimum dosage for the rest of the study and follow-up comprehensive laboratory investigations.

In the case of NS additive studies, all three multiparameter tests on unsoaked strengths (Table 5) indicated that the addition of 0.25% NS does not have any significant influence on the differences of means (*p*-value >0.05). However, the next higher dosage, i.e., 0.5% of NS provided the *p*-value less than 0.05, validating the assumption of a significant difference of mean UCS values between the test groups. From the multiparameter analysis on the retained strengths after capillary soaking, it was observed that all C + L + YNS treated soil groups were able to produce significant difference of means as compared with lime-treated soils (Table 6). However, from the engineering judgment perspective [Fig. 4(c)], it was observed that the 0.5% NS retained maximum strength (47%) after subjecting the specimen to capillary soaking. Therefore, again based on engineering judgment as well as statistical analysis, 0.5% NS was deemed as the optimum dosage for further studies. Subsequent sections present analysis and discussion of results from other engineering tests performed on soils treated with 6% lime and optimum silica dosages, including 0.5% NS and 15% CS.

Accelerated Enhancements in Engineering Properties at Optimum Dosage Conditions

Accelerated Strength Development and Durability Studies

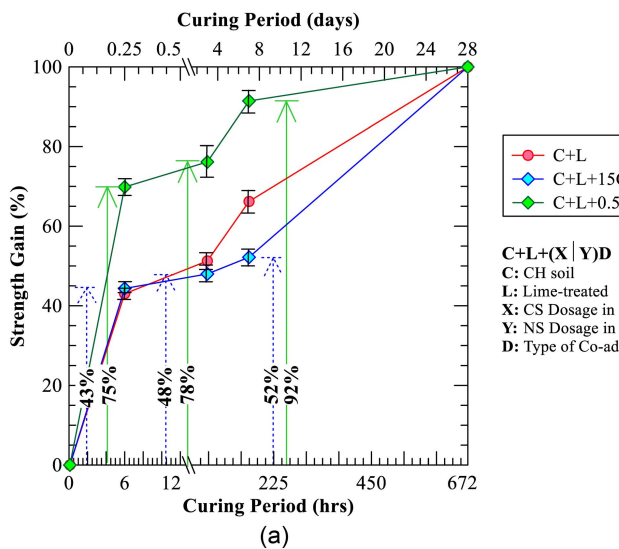
Lime-treated soils continue to gain strength even after several years of treatment; however, a substantial strength gain is generally observed during the first few months after treatment (Townsend and

Donaghe 1976; Little and Nair 2009; Chakraborty and Nair 2020). Therefore, for comparison purposes, the maximum strength of the treated soil was assumed to be that of a 28-day curing period. The 28-day average UCS values of C + L, C + L + 15CS, and C + L + 0.5NS treated soil groups were 753, 823, and 889 kPa, respectively. After seven days of curing, the C + L, C + L + CS, and C + L + NS treated soil groups exhibited average UCS values of 498, 429, and 814 kPa, respectively. The strength gain is plotted as a percentage of the maximum strength (28-day cured strength) for different soil groups and for all three curing periods (zero, three, and seven days) to understand the efficacy of coadditives on accelerated strength gain [Fig. 5(a)].

For the lime-CS treated soil, it could be observed that the percentage of strength gain after seven days is the lowest among all the treated soil groups, even though it has a higher long-term strength after 28 days of curing when compared with lime-treated soil results. This could be attributed to the partial replacement of natural soil silicates and aluminates by the CS additive during initial curing period. The crystalline counterpart from the CS coadditive might have reacted over a longer curing period and formed additional cementitious phases as compared with lime treatment alone.

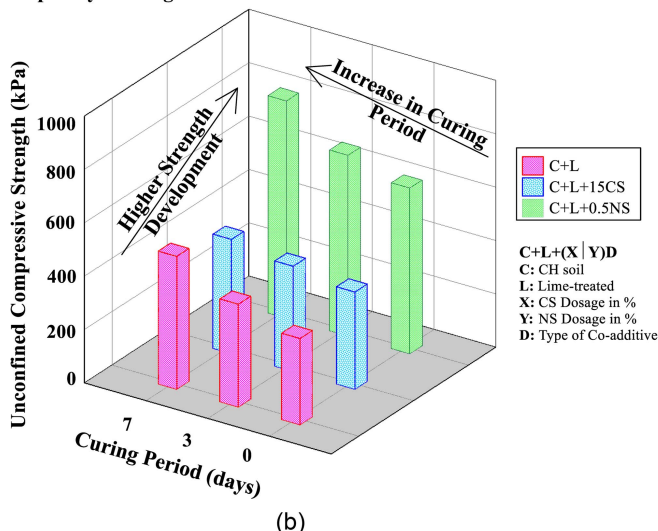
For the NS-treated soil, it could be observed that there is an accelerated development of strength, and it reaches about 90% of the ultimate strength within the first seven days of the treatment. The presence of amorphous nanoparticles provides a large specific surface area ($\sim 140 \text{ m}^2/\text{g}$) for the enhanced chemical reactions between the Ca^{2+} ions from lime and silica particles. The available nanosilica particles in NS-treated soils form the C—S—H phases immediately after the treatment, which is corroborated using micro-studies in the later sections. These factors contribute to the rapid strength gain for the NS-treated soils when compared with lime-treated and lime-CS-treated soils.

The average UCS values of the treated soil groups before and after subjecting the specimens to capillary soaking are shown in Figs. 5(b and c). It was observed that, immediately after the treatment with lime or lime plus coadditives, there is substantial improvement in the UCS property [Fig. 5(b)]. This occurs primarily due to modification reactions among stabilizers and soil particles. Fig. 5(c) shows the average retained strength of the treated specimens when subjected to moisture conditioning for 48 h. From Fig. 5(c), it could be noted that, during the early curing period, there was an appreciable loss of unconfined strength for all treated groups. The pozzolanic reactions are generally a time-dependent phenomenon; as a result, during the early curing periods, there is no substantial development of C—S—H phases, which could provide sufficient bonding to the soil particles (Dash and Hussain 2012; Chakraborty and Nair 2020). Due to moisture intrusion of the treated soils during initial curing period, there is possible weakening of the cementitious bonds, and this may have contributed to the decrease in strength values.



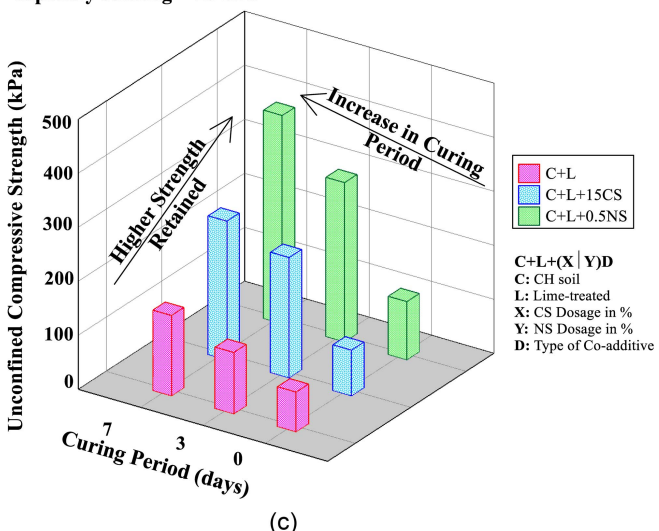
(a)

UCS of untreated specimens before capillary soaking = 232 kPa



(b)

UCS of untreated specimens after capillary soaking = 25 kPa



(c)

Fig. 5. Effect of curing period of different treatments (a) percentage of strength gain with respect to 28 days strength; (b) unsoaked UCS; and (c) UCS after 48 h of capillary soaking.

For the soils treated with lime and coadditives, the strength loss from moisture conditioning is 20% to 30% lower as compared with lime treatment alone. For the CS dosage, percentage loss is minimum because of two possible reasons: (1) partial replacement of clay by crystalline silica; and (2) presence of a higher reactive specific surface area and broken bonds at the edges of the silica particles [J. T. McKennon, "Method for producing enhanced soil stabilization reactions between lime and clay soils due to the effect of silica addition," US Patent No. 5,336,022 (1994); Chakraborty et al. 2022]. Due to these two factors, less water was absorbed by the soil particles, and, subsequently, additional reactive surfaces provided active sites for the formations of cementitious phases, respectively. For the NS-treated soil, a small percentage of dosage provides a significant specific surface area of $140 \text{ m}^2/\text{g}$ of reactive amorphous silica particles uniformly distributed in the soil matrix. These nanosized silica particles provide reactive surfaces and higher potential of chemical reactions with the available Ca^{2+} ions from the Ca-based stabilizer and immediately develop cementitious bonds. These additional C—S—H phases are instrumental

in preventing loss of strength during a shorter curing period after treatment. Microstructural and mineralogical studies discussed here in later sections provided ample proof of the rapid formation of cementitious phases to validate the noted observations in the engineering properties.

Expediting Improvements in Swell–Shrink Performance with Coadditive Treatment

During the initial curing period (≤ 7 days), in addition to the rapid development of strength gains, the application of coadmixtures should improve other engineering properties such as free swell and shrinkage strains. Fig. 6 shows the free swell strains for all soil groups after zero (6 h), three, and seven days of curing. The untreated soil has a free swell strain of 15.6% and could be classified as a problematic high-swelling clay. For serviceability criteria, it is generally expected that, after chemical treatment at a select curing period, the soil should undergo swelling less than 2% to 3%. Fig. 6(a) shows the free swell strain curves immediately (6 h) after treatment. In treated soil specimens, the free swelling strain was

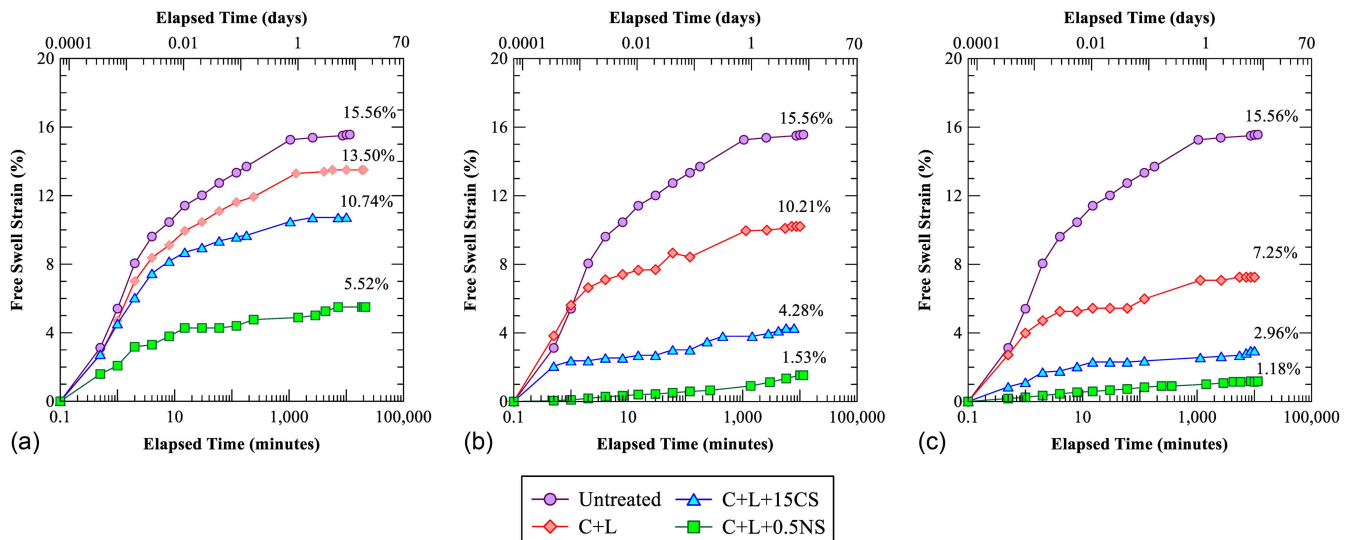


Fig. 6. Free-swell strains of untreated and treated soils after (a) zero (6 h); (b) three; and (c) seven days.

reduced as compared with untreated soil specimens. In lime-treated soil, the modification reactions, including well-established cation exchange and flocculation-agglomeration reactions, are known to be responsible for the observed improvements (Little 1999; Puppala et al. 2016; Chakraborty et al. 2022).

In lime and CS-treated specimens, there was a further reduction in swell strains immediately after the treatment. This could be attributed to two primary reasons: (1) initiation of modification reactions due to the addition of a lime binder to the soil; and (2) partial replacement of high swelling CH soil with a nonswelling crystalline silica counterpart. For the NS-treated soil specimens, adding a small dosage of NS provides a considerable quantity of reactive silica phases, which immediately reacts with the Ca^{+2} ions from lime and forms cementitious compounds. The C-S-H phases formed bonds within the soil matrix and thus prevented the repulsive swelling forces due to moisture intrusion during tests.

The free swell strains of different treated soil groups after three and seven days of curing periods are presented in Figs. 6(b and c). Treated soils showed a lower free swell strain percentage as compared with untreated or zero-day-treated soil specimens. This happens due to the pozzolanic reactions and the formation of cementitious compounds that bond the soil particles together. In the case of the lime and CS-treated specimens, partial replacement of high PI clay with low swelling sand and formation of additional cementitious phases on the broken edges of the admixture helped to reduce the swell percentage values when compared with lime treatments alone. Since the pozzolanic reactions are slow and take place over a longer curing period, this slow rate of reactions has not yielded immediate reductions in free swell strains. When the NS coadditive is added to lime-treated soil, the highly reactive surfaces immediately accelerate the reactions and produce a substantial quantity of cementitious gels. This additional C-S-H phase plus the cementitious compounds from the pozzolanic reactions helped to accelerate the reduction in free swell strains after three and seven days of curing as compared with traditional treatments.

Cyclic swelling and shrinkage strains of expansive soils cause a deleterious impact on civil infrastructure performance. The shrinkage strain of soil from drying is a major contributor of the poor pavement infrastructure, and these properties were evaluated.

Fig. 7 presents the linear shrinkage strains of the untreated and treated soil groups at three curing periods (zero, three, and seven days) to compare the rapid improvements in the shrinkage property due to coadditive applications. The untreated soil has a shrinkage strain of 14.5%, which is recognized as a major problematic soil condition for expansive soils. Adding Ca-based stabilizer to the untreated soil reduced the moisture affinity by neutralizing the surface charges with divalent calcium ions; the resulting treated soil absorbed less water ions and subsequently experience lesser drying of the absorbed water, hence lower shrinkage cracks in the soil.

Inclusion of the CS admixture to the high-PI clay improved the soil shrinkage cracking resistance due to partial replacement of high plastic clay with coarse-grained CS-material. Similar to the CS amendment, NS also helped to improve the linear shrinkage properties of the high PI clay by enhancing the formation of cementitious gels in the treated soil. From Fig. 7, it is noted that the addition of NS immediately helps to reduce the soil shrinkage. Due to the presence of an appreciable quantity of nanosilica particles, the highly reactive amorphous silica forms additional C-S-H phases. This, along with the filler properties of the nanoparticles, helped to form bonds between the soil particles and develop a denser geomaterial matrix, which subsequently prevented it from undergoing considerable shrinkage strains during drying conditions. Therefore, test results indicated that the presence of silica-based coadditives

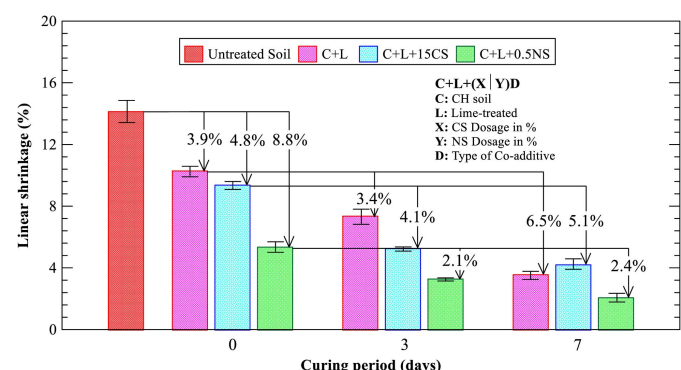


Fig. 7. Linear shrinkage strain for untreated and treated soil specimens.

with a traditional stabilizer expedited the reduction in shrinkage strains of the treated soil matrix.

Influence of Coadditives on Rapid Improvement of Resilient Moduli Properties

The resilient modulus (M_R) from RLTT is a primary input parameter for characterizing the structural support of base and subgrade layers. The advantage of the resilient modulus parameter is its ability to predict pavement distresses such as rutting and cracking using a mechanistic based approach. This test consists of 15 different combinations of confining and deviatoric stresses, representing different stress conditions of a subgrade subjected to different traffic loads. For the ease of representation of the overall influence of all stress state results on moduli of treated soils, resilient properties are represented in the form of universal model constants (Table 7). The universal model constants are obtained from a regression formulation of the respective RLTT data and are represented by the following equation:

$$M_R = k_1 P_a \left(\frac{\theta}{P_a} \right)^{k_2} \left[\left(\frac{\tau_{\text{oct}}}{P_a} \right) + 1 \right]^{k_3} \quad (4)$$

where M_R = the resilient modulus; θ = the bulk stress; τ_{oct} = the octahedral shear stress; P_a = the atmospheric pressure in kPa; and k_1 , k_2 , and k_3 = the universal model parameters. These model parameters were determined from regression analysis of the test data for all treated soil groups. These parameters were used to provide a comprehensive understanding of the influence of treatments on the rapid development of resilient strength.

The k_1 parameter is proportional to the resilient modulus of the specimens. From Table 7, it could be noted that, immediately after lime treatment, the k_1 parameter values are close for lime-treated and C + L + 15CS-treated soil specimens. However, for the NS-treated soil specimens, there is a rapid increase in the parameter immediately after the treatment (6 h). With an increase in the curing period, there was a gradual increase in the resilient moduli for all treated soil groups. Overall, after seven-day curing, the maximum increase in the elastic modulus was observed for the CS-treated soil groups. The presence of crystalline counterparts in the treated soil influenced the improvement in the moduli; for NS, the additional amorphous binding gels within the pore structures increased the overall cohesion and reduced the friction, subsequently affecting the elastic moduli properties.

The k_2 parameter represents the effect of bulk stress on the RLTT values. No definite conclusions could be drawn on the trends of the k_2 parameters in this study. The k_3 parameter represents the effect of the shear stress term on the soil modulus. A negative k_3 value represents a weak soil, as an increase in shear stress reduces the M_R value of the soil. A positive k_3 value with an increase in curing time period represents a strain hardening effect, a typical characteristic of treated soil materials. For the C + L- and C + L + 15CS-treated soil groups, the rate of increase in the k_3 value was lower when compared with those of the C + L + 0.5NS soils.

This represents that the presence of NS accelerates the resistance against the shear stresses when compared with lime and CS or only lime-treated specimens. Therefore, at the end of seven days of the curing period, although the overall resilient modulus of the soil groups treated with NS was lower than the rest of the treated soil groups, the improvement in strain hardening effect was higher than the other treatment techniques.

Therefore, based on the strength studies before and after the capillary soaking process in the previous section, as well as the resilient moduli studies here, an important finding was noted, i.e., the NS provided considerable strength enhancements during the early curing periods than the moduli enhancements; further, this variation is attributed to the size and composition of NS particles and related pozzolanic compounds. Observations on the effects of CS and NS on accelerating the engineering performance of expansive soils needed further verification and validation; as a result, microsoil behavior studies were performed on the treated soils. The next section discusses microstructural studies results to link between micro- and macrobehavior of CS- and NS-treated soils.

Mineralogical and Microstructural Influence on Accelerated Treatments

The effects of coadditives when mixed with a traditional stabilizer were analyzed using microstructural studies. The FESEM was performed to study the differences in the morphological changes that occurred due to different treatments, as shown in Fig. 8. Figs. 8(a and b) present the untreated soil at 1,000 \times and 2,000 \times magnification, respectively. The SEM image at 1,000 \times shows the honeycomb structures typically observed in clayey soils. With further magnification (2,000 \times), it could be noted that there is a substantial amount of small flaky to rounded shaped particles with open-pore structures. Figs. 8(c and d) show the images of seven-day cured C + L + 15CS-treated specimens under 1,000 \times and 2,700 \times , respectively. The addition of lime and CS additives helps to form cementitious compounds, which provide additional bonds to improve the soil properties. The SEM image at higher magnification (2,700 \times) reveals globular cementitious phases formed at the edges of the soil particles. The presence of these cementitious phases helped to retain strength after being subjected to the capillary soaking process and subsequently prevented volumetric strains in the treated soil specimens, as compared with the untreated soil [Figs. 5(c) and 6].

The soil specimen treated with lime and NS binders and cured for seven days is shown in Figs. 8(e and f). Under 2,000 \times magnification, it could be noted that the soil particles are coated with a uniform matrix of C—S—H phases due to the NS treatment as well as the open voids, which are filled up due to the addition of nanoparticles. The addition of NS helps to develop cementitious products, which provides a strong soil matrix. These additional cementitious phases, along with the time-dependent pozzolanic reactions, could have provided rapid enhancement in the engineering properties, as observed in the previous sections (Figs. 5–7).

Table 7. Universal model parameters from resilient modulus (M_R) test

Curing Period (days)	k_1			k_2			k_3			R^2		
	C + L	C + L + 15CS	C + L + 0.5NS	C + L	C + L + 15CS	C + L + 0.5NS	C + L	C + L + 15CS	C + L + 0.5NS	C + L	C + L + 15CS	C + L + 0.5NS
0	1,426.34	1,469.83	1,746.84	0.159	0.174	0.092	-0.926	-0.755	0.138	0.92	0.95	0.94
3	1,868.56	1,758.51	1,801.81	0.151	0.144	0.257	-0.201	0.215	0.307	0.86	0.91	0.94
7	1,859.20	2,088.03	1,822.01	0.143	0.119	0.180	0.340	0.657	0.541	0.89	0.95	0.90

Note: k_1 , k_2 , and k_3 are the universal model parameters.

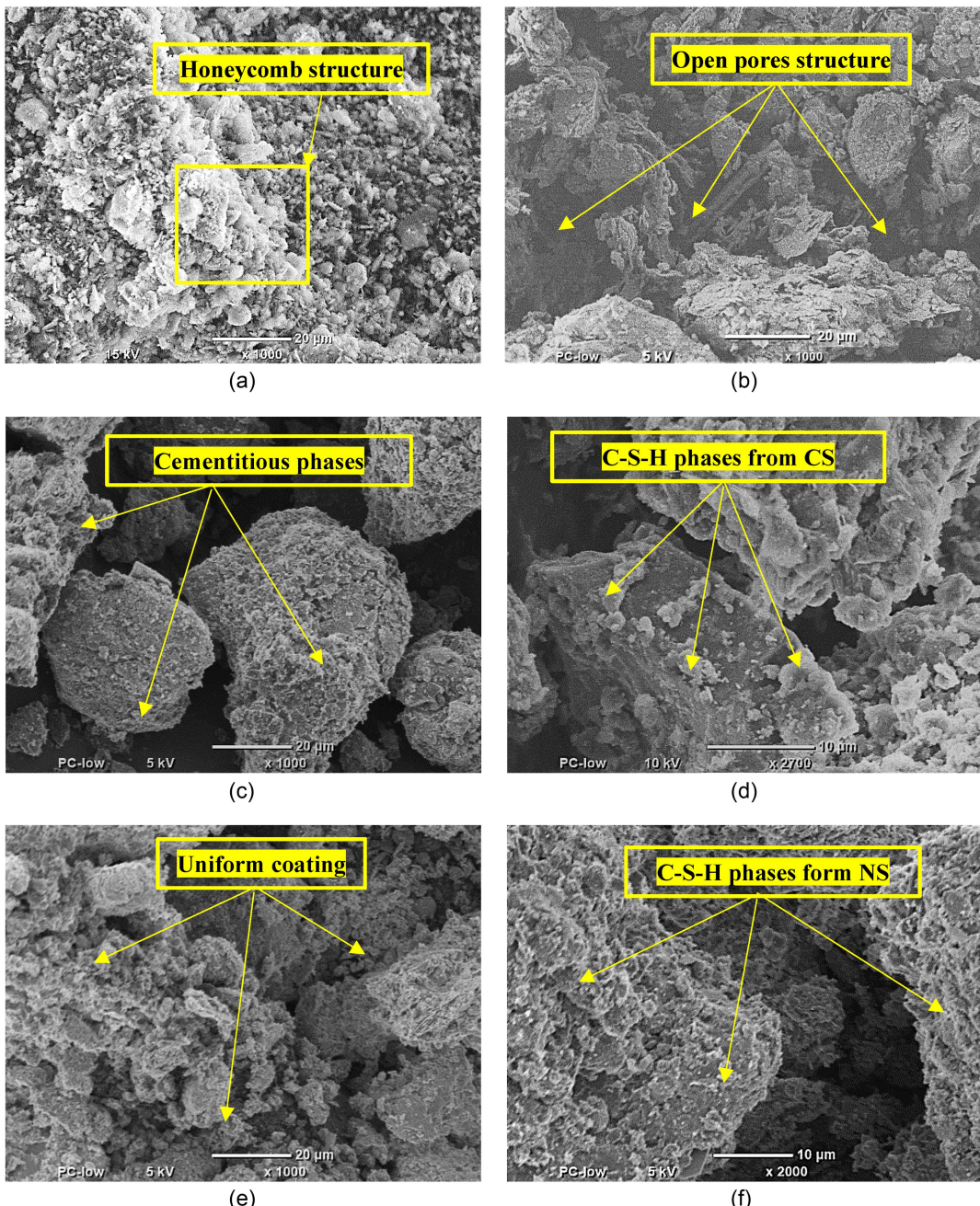


Fig. 8. FESEM images under different magnification (a) untreated soil (1,000 \times); (b) untreated soil (2,000 \times); (c) C + L + 15CS (1,000 \times); (d) C + L + 15CS (2,700 \times); (e) C + L + 0.5NS (1,000 \times); and (f) C + L + 0.5NS (2,000 \times).

However, from the SEM images, no conclusive proof was obtained regarding the accelerated chemical reactions. To verify the hypothesis, XRD studies on the silica-based coadditives with lime are presented in the following to provide evidence of accelerated chemical reactions.

Fig. 9 represents the x-ray diffractograms for the two different coadmixtures treated with dolomitic hydrated lime. The XRD patterns of an untreated NS and CS coadditives are shown in Figs. 9(a and b). Being amorphous in nature, no definitive peak was observed in the NS powder; rather, a characteristic hump associated with amorphous compounds can be observed between 2θ values of 20° to 25°. The CS showed primarily the quartz peaks at 20.84°, 26.63°, 36.51°, 39.47°, 42.41°, 50.12°, and 59.91° and some feldspar peaks at 13.66°, 27.11°, and 27.59°. Since the quartz

sand-based CS was obtained from a natural source, the presence of feldspar was observed, possibly due to the mineral stability and genesis from the parent rock.

Immediately after the addition of the lime dosage to the NS and CS coadditives, a number of new peaks were observed in the diffractograms. The primary peaks of portlandite $[\text{Ca}(\text{OH})_2]$ and brucite $[\text{Mg}(\text{OH})_2]$ were observed due to their presence in the Ca-based stabilizer. The characteristic calcite peaks were observed due to the partial carbonation of the hydrated lime in the presence of CO_2 from the surrounding atmosphere. Since the reactions were not conducted in a nitrogen-controlled environment to simulate actual field situations, substantial calcite formation was noted with the progress of the reactions. Immediately after the addition of lime to NS, some cementitious C-S-H phases were observed, which

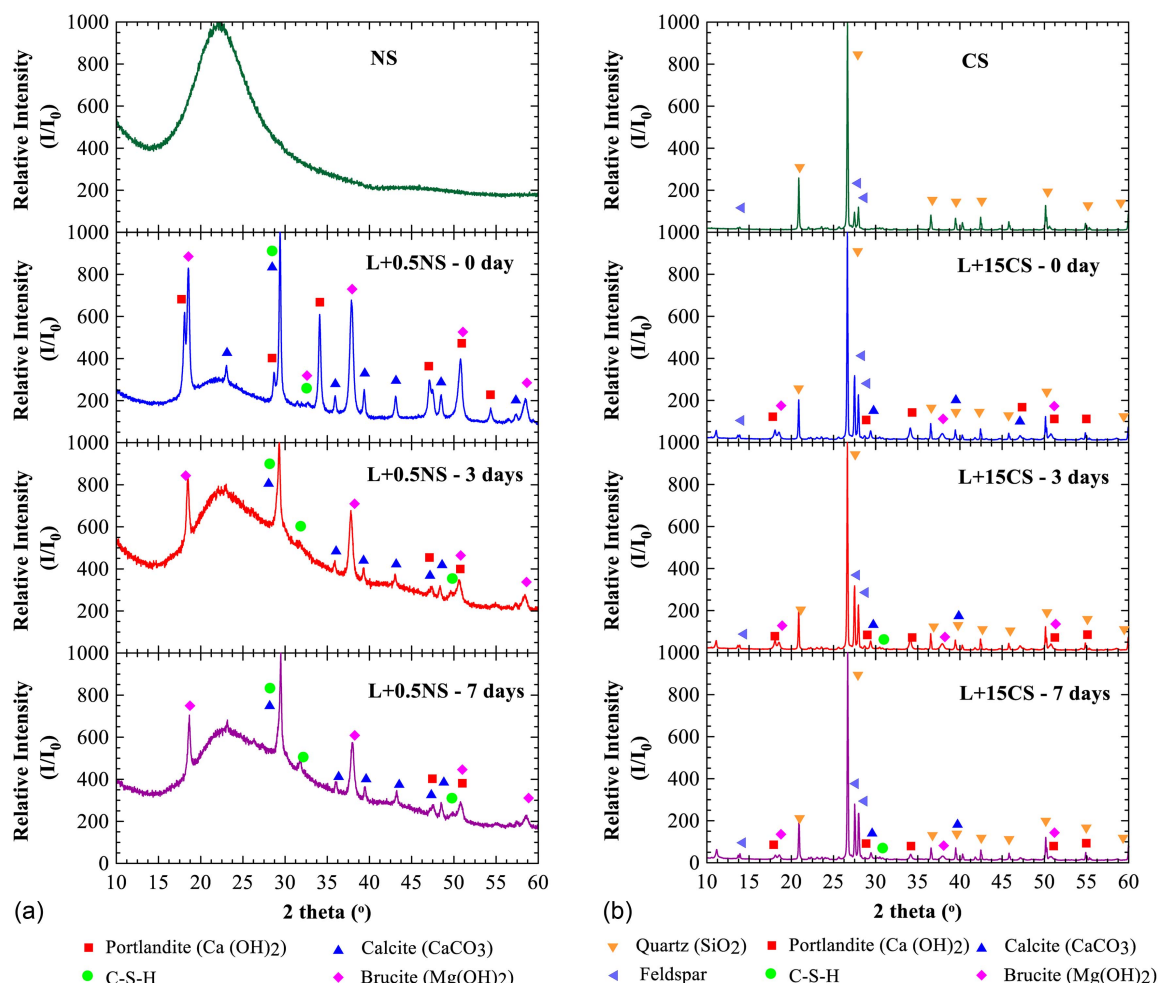


Fig. 9. XRD pattern over different curing periods for specimens of lime mixed with silica-based coadditives: (a) nanosilica; and (b) crystalline silica.

are visible from peaks ranging between 31° and 32° in the diffractograms (He et al. 2011; Chakraborty and Nair 2020). These peaks developed from the immediate precipitation of C-S-H phases due to rapid reactions between the portlandite and NS. The relative intensity of the amorphous hump is significantly low on zero day because of the presence of a major portion of crystalline compounds from the dolomitic lime. In contrast, no immediate changes were distinctly visible in the CS and lime-treated soil specimen diffractogram.

After three days of curing, in the lime and NS-treated specimens, none of the portlandite peaks were visible. Portlandite, being more soluble than brucite, releases Ca^{+2} ions, which reacts with the available amorphous NS powders and form C-S-H phases. Distinct C-S-H peaks at 31.86° and 49.71° are noted after three days of treatment, corroborating the observations. Additionally, it was also observed that there was no relative increase in the calcite peaks during the same period, indicating that the majority of Ca^{+2} was used to form C-S-H phases rather than carbonation reactions. After seven days of curing, a relative reduction in the brucite peaks was observed as compared with the three-day curing period (e.g., $2\theta = 18.55^\circ$, the counts reduced from 6,245 at three days to 5,793 counts at seven). Additionally, a distinct C-S-H peak is visible at 31.86° confirming the formation of C-S-H gels rapidly in the presence of NS and dolomitic hydrated lime. Furthermore, it was observed that the relative intensity of the amorphous hump

increased over curing period, indicating the maximum utilization of the crystalline compounds in the stabilizer to form amorphous cementitious C-S-H phases. This rapid formation of the C-S-H phases provides additional sources of cementitious gels in addition to the pozzolanic reactions from the lime-soil reactions and helps to quickly improve the engineering properties during the early curing period (Figs. 5–7).

Lime and CS-treated specimens show no rapid changes immediately after the early curing period. After three and seven days of curing, most of the portlandite and brucite peaks were visible in the diffractogram. At the end of seven-days curing, it was observed that there was a decrease in the relative intensity of the portlandite peaks at 18.08° and 34.11° , along with a number of visible amorphous peaks of C-S-H between 31° and 32° in the diffractograms. This indicates chemical reactions between the crystalline silica co-additive and the calcium ions, which produces cementitious phases. These cementitious phases are responsible for providing additional strength at the end of a longer curing period (28 days).

From the microstudies, it was noted that, during the early curing period, the precipitation of cementitious phases produced by amorphous NS was faster in comparison with the CS co-additive. These phases were responsible for the observed accelerated improvements in the engineering properties such as strength, durability, swell-shrink, and resilient modulus properties. CS co-additives are crystalline in nature and react through active sites at the edges with

broken bonds, whereas NS, being amorphous in nature, consists of a high-specific surface area of reactive silica, which, when treated with lime, immediately precipitates additional cementitious phases. Therefore, considering engineering aspects and microstructural studies, the application of NS was observed to be more effectual than CS in rapidly improving the engineering properties of the problematic high-plastic clays.

Conclusions and Recommendations

A comprehensive laboratory investigation was undertaken to study the effects of silica-based coadditives in accelerating the improvements in engineering properties of problematic soils when mixed with traditional Ca-based stabilizers. Two silica-based coadditives, crystalline silica or CS and nanosilica or NS, were extensively studied, and their efficacy in stabilization performance was compared for early curing periods. Optimization of the coadditive dosages was performed based on one- and two-parameter analyses of seven-day unconfined compression strength and durability characteristics. Based on the optimum dosages established, an array of other prominent performance-based engineering tests, including linear swell, shrinkage, unconfined strength, and durability, as well as resilient moduli studies, were performed over three early curing periods of zero, three, and seven days. Microstructural studies using FESEM and XRD were also performed to gain insights into the reasons for the accelerated formation of cementitious products. Some of the salient findings from the research are presented later in this text.

Silica-based coadditives have a significant influence on modifying the properties of expansive soils when added with dolomitic-hydrated lime. The CS rich quarry dust fines possess a higher specific surface and significant broken bonds near the edges due to their microparticle size. These enhance the development of additional cementitious phases when mixed with traditional stabilizers. Laboratory-grade NS-based coadditive consists of nanoparticles, which provides substantial reactive surfaces to form additional bonding gels when added along with lime. The optimization of CS and NS coadditive dosages was based on seven-day unconfined strength and durability studies of CS or NS mixed with a primary stabilizer. Based on statistical analysis using one-parameter and multiparameter studies, dosages of 15% of CS and 0.5% of NS were determined as optimum dosages with 6% lime.

The NS coadditive has a significant influence on rapidly accelerating the strength, durability, free swell, and shrinkage of the treated soil within the first three days of curing period. CS coadditives improve the long-term performance of the treated soil as compared with lime treatment alone; however, it has a negligible influence on rapidly developing the engineering properties during the first seven days of the curing process. The particle size and the available specific reaction surfaces of the individual coadditives could be attributed as some of the reasons for these changes in soil behaviors. The resilient moduli properties of the CS-treated soils were observed to be moderately higher than the NS soils due to more interparticular friction from CS materials.

Microstructural studies indicated that CS- and NS-treated soils are helpful to form additional C—S—H phases uniformly distributed in the treated soil. The XRD studies on the coadditives mixed with lime showed that the portlandite gets rapidly used up when mixed with NS and leads to the development of new C—S—H peaks. This indicates the efficacy of using NS for accelerating the formation of cementitious phases in the treated soils where rapid property enhancements are needed in early curing periods. Overall, the research study provides a comprehensive understanding of novel silica-based coadditives to improve the treated soil properties

rapidly. Civil infrastructure and transportation agencies could significantly benefit from using these coadditives for accelerating stabilization improvements of subsoils, thereby providing resilient foundation systems. However, it should be noted that the embodied energy during the production stages of the novel materials and the cost of pure-grade silica-based coadditives are significantly high. Therefore, comprehensive life-cycle cost analyses and sustainability benefit analyses are recommended before application into actual projects. Additionally, future field studies are necessary to validate the efficacy of these silica treatments, which will be valuable in the utilization of silica additives for calcium-based treatments.

Data Availability Statement

Some or all data, models, or code that support the findings of this study are available from the corresponding author upon reasonable request.

Acknowledgments

This work was also made possible in part by NSF Industry-University Cooperative Research Center (I/UCRC) program funded Center for Integration of Composites into Infrastructure (CICI) site at Texas A&M University, NSF PD: Dr. Prakash Balan; Award #2017796. The authors would also like to thank Mr. Krishneshwar Ramineni for his help with microstructural tests at CIR.

References

- AASHTO. 1993. *Guide for design of pavement structures*. Washington, DC: AASHTO.
- AASHTO. 2003. *Standard method of test for determining the resilient modulus of soils and aggregate materials*. AASHTO T 307. Washington, DC: AASHTO.
- Aldaoood, A., M. Bouasker, and M. Al-Mukhtar. 2014. “Geotechnical properties of lime-treated gypseous soils.” *Appl. Clay Sci.* 88–89 (Feb): 39–48. <https://doi.org/10.1016/j.clay.2013.12.015>.
- Al-Rawas, A. A., and M. F. A. Goosen. 2006. *Expansive soils: Recent advances in characterization and treatment*. London: Taylor & Francis.
- ASTM. 2010. *Standard test methods for moisture-density (Unit Weight) relations of soil-cement mixtures*. ASTM D558-04. West Conshohocken, PA: ASTM.
- ASTM. 2016. *Standard test methods for specific gravity of soil solids by water pycnometer*. ASTM D854-14. West Conshohocken, PA: ASTM.
- ASTM. 2018a. *Standard specification for quicklime and hydrated lime for soil stabilization*. ASTM C977-18. West Conshohocken, PA: ASTM.
- ASTM. 2018b. *Standard test method for unconfined compressive strength of compacted soil-lime mixtures (Withdrawn 2018)*. ASTM D5102-09. West Conshohocken, PA: ASTM.
- ASTM. 2018c. *Standard test methods for liquid limit, plastic limit, and plasticity index of soils*. ASTM D4318-17e1. West Conshohocken, PA: ASTM.
- ASTM. 2019. *Standard test method for using pH to estimate the soil-lime proportion requirement for soil stabilization*. ASTM D6276-19. West Conshohocken, PA: ASTM.
- ASTM. 2020. *Standard practice for classification of soils for engineering purposes (Unified Soil Classification System)*. ASTM D2487-17. West Conshohocken, PA: ASTM.
- ASTM. 2021a. *Standard test method for particle-size distribution (Gradation) of fine-grained soils using the sedimentation (hydrometer) analysis*. ASTM D7928-21e1. West Conshohocken, PA: ASTM.

ASTM. 2021b. *Standard test methods for laboratory compaction characteristics of soil using standard effort (12,400 ft-lbf/ft³ (600 kN-m/m³)).* ASTM D698-12. West Conshohocken, PA: ASTM.

ASTM. 2021c. *Standard test methods for one-dimensional swell or collapse of soils.* ASTM D4546-21. West Conshohocken, PA: ASTM.

Bahmani, S. H., N. Farzadnia, A. Asadi, and B. B. K. Huat. 2016. "The effect of size and replacement content of nanosilica on strength development of cement treated residual soil." *Constr. Build. Mater.* 118 (Aug): 294–306. <https://doi.org/10.1016/j.conbuildmat.2016.05.075>.

Bahmani, S. H., B. B. K. Huat, A. Asadi, and N. Farzadnia. 2014. "Stabilization of residual soil using SiO₂ nanoparticles and cement." *Constr. Build. Mater.* 64 (Jul): 350–359. <https://doi.org/10.1016/j.conbuildmat.2014.04.086>.

Bakharev, T., J. G. Sanjayan, and Y.-B. Cheng. 1999. "Effect of elevated temperature curing on properties of alkali-activated slag concrete." *Cem. Concr. Res.* 29 (10): 1619–1625. [https://doi.org/10.1016/S0008-8846\(99\)00143-X](https://doi.org/10.1016/S0008-8846(99)00143-X).

Behnood, A. 2018. "Soil and clay stabilization with calcium- and non-calcium-based additives: A state-of-the-art review of challenges, approaches and techniques." *Transp. Geotech.* 17 (Mar): 14–32. <https://doi.org/10.1016/j.trgeo.2018.08.002>.

Bell, F. G. 1996. "Lime stabilization of clay minerals and soils." *Eng. Geol.* 42 (4): 223–237. [https://doi.org/10.1016/0013-7952\(96\)00028-2](https://doi.org/10.1016/0013-7952(96)00028-2).

Biswas, N., A. J. Puppala, S. Chakraborty, and M. A. Khan. 2021. "Utilization of silica-based admixture to improve the durability of lime-treated expansive soil." In *Proc., IFCEE 2021*, 233–242. Reston, VA: ASCE.

Brough, A., and A. Atkinson. 2002. "Sodium silicate-based, alkali-activated slag mortars." *Cem. Concr. Res.* 32 (6): 865–879. [https://doi.org/10.1016/S0008-8846\(02\)00717-2](https://doi.org/10.1016/S0008-8846(02)00717-2).

Chakraborty, S., and S. Nair. 2017. "Impact of different hydrated cementitious phases on moisture-induced damage in lime-stabilised subgrade soils." *Road Mater. Pavement Des.* 19 (6): 1389–1405. <https://doi.org/10.1080/14680629.2017.1314222>.

Chakraborty, S., and S. Nair. 2020. "Impact of curing time on moisture-induced damage in lime-treated soils." *Int. J. Pavement Eng.* 21 (2): 215–227. <https://doi.org/10.1080/10298436.2018.1453068>.

Chakraborty, S., A. J. Puppala, and N. Biswas. 2022. "Role of crystalline silica admixture in mitigating ettringite-induced heave in lime-treated sulfate-rich soils." *Géotechnique* 72 (5): 438–454. <https://doi.org/10.1680/jgeot.20.P.154>.

Chen, R., V. P. Drnevich, and R. K. Daita. 2009. "Short-term electrical conductivity and strength development of lime kiln dust modified soils." *J. Geotech. Geoenvir. Eng.* 135 (4): 590–594. [https://doi.org/10.1061/\(ASCE\)1090-0241\(2009\)135:4\(590\)](https://doi.org/10.1061/(ASCE)1090-0241(2009)135:4(590).

Chittoori, B. C. S. 2008. "Clay mineralogy effects on long-term performance of chemically treated expansive clays." Ph.D. thesis, Dept. of Civil and Environmental Engineering, Univ. of Texas at Arlington.

Chittoori, B. C. S., A. J. Puppala, T. Wejrungskul, and L. R. Hoyos. 2013. "Experimental studies on stabilized clays at various leaching cycles." *J. Geotech. Geoenvir. Eng.* 139 (10): 1665–1675. [https://doi.org/10.1061/\(ASCE\)GT.1943-5606.0000920](https://doi.org/10.1061/(ASCE)GT.1943-5606.0000920).

Christopher, B. R., C. W. Schwartz, R. Boudreaux, and R. R. Berg. 2006. *Geotechnical aspects of pavements.* NHI Course No.132040. Washington, DC: Federal Highway Administration.

Çokça, E. 2001. "Use of class c fly ashes for the stabilization of an expansive soil." *J. Geotech. Geoenvir. Eng.* 127 (7): 568–573. [https://doi.org/10.1061/\(ASCE\)1090-0241\(2001\)127:7\(568\)](https://doi.org/10.1061/(ASCE)1090-0241(2001)127:7(568).

Das, J. T. 2018. *Assessment of sustainability and resilience in transportation infrastructure geotechnics.* Arlington, TX: Univ. of Texas at Arlington.

Dash, S. K., and M. Hussain. 2012. "Lime stabilization of soils: Reappraisal." *J. Mater. Civ. Eng.* 24 (6): 707–714. [https://doi.org/10.1061/\(ASCE\)MT.1943-5533.0000431](https://doi.org/10.1061/(ASCE)MT.1943-5533.0000431).

Dempsey, B. J., and M. R. Thompson. 1968. *Durability properties of lime-soil mixtures.* Washington, DC: Highway Research Record.

Dhar, S., and M. Hussain. 2021. "The strength and microstructural behavior of lime stabilized subgrade soil in road construction." *Int. J. Geotech. Eng.* 15 (4): 471–483. <https://doi.org/10.1080/19386362.2019.1598623>.

Givi, A. N., S. A. Rashid, F. N. A. Aziz, and M. A. M. Salleh. 2013. "Influence of 15 and 80 nano-SiO₂ particles addition on mechanical and physical properties of ternary blended concrete incorporating rice husk ash." *J. Exp. Nanosci.* 8 (1): 1–18. <https://doi.org/10.1080/17458080.2010.548834>.

Gomes Correia, A., M. G. Winter, and A. J. Puppala. 2016. "A review of sustainable approaches in transport infrastructure geotechnics." *Transp. Geotech.* 7 (Aug): 21–28. <https://doi.org/10.1016/j.trgeo.2016.03.003>.

Han, Z., and S. K. Vanapalli. 2016. "Stiffness and shear strength of unsaturated soils in relation to soil-water characteristic curve." *Géotechnique* 66 (8): 627–647. <https://doi.org/10.1680/jgeot.15.P.104>.

He, Y., X. Zhao, L. Lu, L. J. Struble, and S. Hu. 2011. "Effect of C/S ratio on morphology and structure of hydrothermally synthesized calcium silicate hydrate." *J. Wuhan Univ. Technol. Mater. Sci. Ed.* 26 (4): 770–773. <https://doi.org/10.1007/s11595-011-0308-z>.

Hilbig, H., and A. Buchwald. 2006. "The effect of activator concentration on reaction degree and structure formation of alkali-activated ground granulated blast furnace slag." *J. Mater. Sci.* 41 (19): 6488–6491. <https://doi.org/10.1007/s10853-006-0755-7>.

Ingalkar, R. S., and S. M. Harle. 2017. "Replacement of natural sand by crushed sand in the concrete." *Landscape Archit. Reg. Plann.* 2 (1): 13–22. <https://doi.org/10.11648/j.larp.20170201.12>.

Jang, J., A. J. Puppala, S. Chakraborty, N. Biswas, O. Huang, and M. Radovic. 2021. "Eco-Friendly stabilization of sulfate-rich expansive soils using geopolymers for transportation infrastructure." In *Proc., Tran-SET 2021*, 223–231. Reston, VA: ASCE.

Kennedy, T. W., R. Smith, R. J. Holmgreen Jr., and M. Tahmoressi. 1987. "An evaluation of lime and cement stabilization." *Transp. Res. Board* 1119 (1): 11–25.

Khan, M. A., N. Biswas, A. Banerjee, and A. J. Puppala. 2020. "Field performance of geocell reinforced recycled asphalt pavement base layer." *Transp. Res. Rec.* 2674 (3): 69–80. <https://doi.org/10.1177/0361198120908861>.

Kukko, H. 2000. "Stabilization of clay with inorganic by-products." *J. Mater. Civ. Eng.* 12 (4): 307–309. [https://doi.org/10.1061/\(ASCE\)0899-1561\(2000\)12:4\(307\)](https://doi.org/10.1061/(ASCE)0899-1561(2000)12:4(307).

Kumar, A., and D. Gupta. 2016. "Behavior of cement-stabilized fiber-reinforced pond ash, rice husk ash-soil mixtures." *Geotext. Geomembr.* 44 (3): 466–474. <https://doi.org/10.1016/j.geotexmem.2015.07.010>.

Kumar, A., B. S. Walia, and A. Bajaj. 2007. "Influence of fly ash, lime, and polyester fibers on compaction and strength properties of expansive soil." *J. Mater. Civ. Eng.* 19 (3): 242–248. [https://doi.org/10.1061/\(ASCE\)0899-1561\(2007\)19:3\(242\)](https://doi.org/10.1061/(ASCE)0899-1561(2007)19:3(242).

Lamb, M. J. 2005. *Design guide for applications of sandstone quarry sand in South Wales.* Viridis Rep. No. VR8. Berks, UK: TRL.

Li, W., Y. Yi, and A. J. Puppala. 2019. "Utilization of carbide slag-activated ground granulated blast furnace slag to treat gypseous soil." *Soils Found.* 59 (5): 1496–1507. <https://doi.org/10.1016/j.sandf.2019.06.002>.

Little, D., E. Males, J. Prusinski, and B. Stewart. 2000. "Cementitious stabilization." In *Transportation in the millennium.* Washington, DC: Transportation Research Board.

Little, D. N. 1996. *Evaluation of resilient and strength properties of lime-stabilized soils for the Denver, Colorado area.* Fort Worth, TX: Chemical Lime Company.

Little, D. N. 1999. *Evaluation of structural properties of lime stabilized soils and aggregates—Volume 1: Summary of findings.* Arlington, VA: National Lime Association.

Little, D. N. 2000. *Evaluation of structural properties of lime stabilized soils and aggregates Volume 3: Mixture design and testing procedure for lime stabilized soils.* Arlington, VA: National Lime Association.

Little, D. N., and S. Nair. 2009. *Recommended practice for stabilization of sulfate-rich subgrade soils.* Washington, DC: Transportation Research Board.

McCallister, L. D., and T. M. Petry. 1992. "Leach tests on lime-treated clays." *Geotech. Test. J.* 15 (2): 106–114. <https://doi.org/10.1520/GTJ10232J>.

Misra, A. 1998. "Stabilization characteristics of clays using class c fly ash." *Transp. Res. Rec.* 1611 (1): 46–54. <https://doi.org/10.3141/1611-06>.

Mitchell, J. K., and K. Soga. 2005. *Fundamentals of soil behavior*. New York: Wiley.

National Lime Association. 2004. *Lime-treated soil construction manual: Lime stabilization and lime modification*. Arlington, VA: National Lime Association.

Peethamparan, S., J. Olek, and S. Diamond. 2008. "Physicochemical behavior of cement kiln dust-treated kaolinite clay." *Transp. Res. Rec.* 2059 (1): 80–88. <https://doi.org/10.3141/2059-09>.

Puppala, A., L. Mohammad, and A. Allen. 1996. "Engineering behavior of lime-treated Louisiana subgrade soil." *Transp. Res. Rec.* 1546 (1): 24–31. <https://doi.org/10.1177/0361198196154600103>.

Puppala, A. J. 2021. "Performance evaluation of infrastructure on problematic expansive soils: Characterization challenges, innovative stabilization designs, and monitoring methods." *J. Geotech. Geoenvir. Eng.* 147 (8): 04021053. [https://doi.org/10.1061/\(ASCE\)GT.1943-5606.0002518](https://doi.org/10.1061/(ASCE)GT.1943-5606.0002518).

Puppala, A. J., and A. Pedarla. 2017. "Innovative ground improvement techniques for expansive soils." *Innovative Infrastruct. Solutions* 2 (1): 24. <https://doi.org/10.1007/s41062-017-0079-2>.

Puppala, A. J., A. Pedarla, and A. Gaily. 2016. *Implementation: Mitigation of high sulfate soils in Texas: Development of design and construction guidelines*, 1–39. Austin, TX: Texas DOT.

Puppala, A. J., S. Saride, and R. Williammee. 2012. "Sustainable reuse of limestone quarry fines and RAP in pavement base/Subbase layers." *J. Mater. Civ. Eng.* 24 (4): 418–429. [https://doi.org/10.1061/\(ASCE\)MT.1943-5533.0000404](https://doi.org/10.1061/(ASCE)MT.1943-5533.0000404).

Sivapullaiah, P. V., and A. A. B. Moghal. 2011. "Role of gypsum in the strength development of fly ashes with lime." *J. Mater. Civ. Eng.* 23 (2): 197–206. [https://doi.org/10.1061/\(ASCE\)MT.1943-5533.0000158](https://doi.org/10.1061/(ASCE)MT.1943-5533.0000158).

Sobolev, K., I. Flores, L. M. Torres-Martinez, P. L. Valdez, E. Zarazua, and E. L. Cuellar. 2009. "Engineering of SiO₂ nanoparticles for optimal performance in nano cement-based materials." In *Nanotechnology in construction* 3, 139–148. Berlin: Springer.

Stefanidou, M., and I. Papayianni. 2012. "Influence of nano-SiO₂ on the Portland cement pastes." *Composites, Part B* 43 (6): 2706–2710. <https://doi.org/10.1016/j.compositesb.2011.12.015>.

Taha, M. R., and O. M. E. Taha. 2012. "Influence of nanomaterial on the expansive and shrinkage soil behavior." *J. Nanopart. Res.* 14 (10): 1190. <https://doi.org/10.1007/s11051-012-1190-0>.

Texas DOT. 1999. *Test procedure for determining the bar linear shrinkage of soils*. Tex-107-E. Austin, TX: Texas DOT.

Texas DOT. 2005. *Test procedure for determining sulfate content in soils—Colorimetric method*. Tex-145-E. Austin, TX: Texas DOT.

Townsend, F. C., and R. T. Donaghe. 1976. *Investigation of accelerated curing of soil-lime and lime-fly ash-aggregate mixtures*. Vicksburg, MS: Soils and Pavements Laboratory (US).

Wild, S., J. M. Kinuthia, G. I. Jones, and D. D. Higgins. 1999. "Suppression of swelling associated with ettringite formation in lime stabilized sulphate bearing clay soils by partial substitution of lime with ground granulated blast furnace slag (GGBS)." *Eng. Geol.* 51 (4): 257–277. [https://doi.org/10.1016/S0013-7952\(98\)00069-6](https://doi.org/10.1016/S0013-7952(98)00069-6).